A computational acoustic field reconstruction process based on an indirect boundary element formulation

Zhidong Zhang and Nickolas Vlahopoulos
Department of Naval Architecture and Marine Engineering, The University of Michigan, 2600 Draper Road, Ann Arbor, Michigan 48109-2145

S. T. Raveendra
Automated Analysis Corporation, 2805 South Industrial, Suite 100, Ann Arbor, Michigan 48104-6767

T. Allen
Scientific Research Laboratories, Ford Motor Company, 20000 Rotunda Drive, Building SRL MD2636, Dearborn, Michigan 48121

K. Y. Zhang
Truck VC CAE Department, Advanced Vehicle Technology, Ford Motor Company, 20901 Oakwood Boulevard, MD299, P.O. Box 2053, Dearborn, Michigan 48121

(Received 24 March 2000; revised 10 August 2000; accepted 16 August 2000)

The objective of the work presented in this paper is to develop a computational capability based on the indirect boundary element method (IBEM) for evaluating appropriate velocity boundary conditions on an assembly of piston type sources in order to recreate a prescribed acoustic field. Information for the acoustic pressure of the original acoustic field at certain field points constitutes the input to the developed process. The velocities on the piston type sources are computed from transfer functions evaluated between the field points where the acoustic pressure of the original field is prescribed and the velocity boundary condition on each element of the generic source. The IBEM is employed for computing the transfer functions in order to accommodate the presence of openings in the model and radiation from both sides of the piston type sources. Simulating the generic source as a thin surface that radiates from both sides eliminates the presence of irregular frequencies in the analysis. A singular value decomposition (SVD) solver is integrated with the IBEM computations in order to evaluate the velocity boundary conditions from the transfer functions. The number of field points where the acoustic pressure is defined can be considerably smaller than the number of elements where the velocity is computed. The solution that demonstrates the smallest magnitude is selected from all possible solutions. An algorithm is also developed for identifying the optimum field points where the acoustic pressure of the original field must be prescribed. The optimum field points are selected from a set of prescribed candidate points. The number of optimum points is considered smaller than the number of elements where the velocity is computed. The properties of the transformation matrix and the quality of the reconstruction depend on the location of the field points. Thus, the selection of the optimum points is based on achieving the highest possible orthogonality among the vectors that comprise the range of the transformation matrix. Several validation and application cases are presented.
[S0001-4966(00)04611-7]

PACS numbers: 43.40.Rj [CBB]

I. INTRODUCTION

Several developments have been presented in the past in the area of reconstructing a noise source from acoustic field data. A fast Fourier transform algorithm has been utilized in reconstructing the acoustic field created by sources with simple geometry (planar or cylindrical).[1–3] Green's functions that satisfy a homogeneous condition on the source surface must be available for this development. Thus, the process is applicable only to sources with simple geometry.[1–3] A technique based on the direct boundary element method for identifying a noise source was presented, and the effect of the presence of random error in the field measurements was investigated.[4] Other acoustic holography techniques also based on the direct boundary element method were developed for reconstructing sources with irregular geometry.[5–8] A singular value decomposition (SVD) algorithm was utilized for evaluating velocity on the surface of the vibrating object from the acoustic field data.[5–8] The concept of integrating the direct boundary element method with a SVD algorithm for a source reconstruction was utilized for both exterior radiation[5,6,8] and interior acoustics.[7] Results for sound sources such as a pulsating sphere, a vibrating piston on a rigid sphere, a pulsating cylinder with spherical end caps, and a flexible panel in a baffle have been used for validation.[6,8] Other efforts in the area of acoustic field reconstruction were associated with the development of a Helmholtz equation least squares (HELS) method for the reconstruction of the surface pressure field on sources of irregular

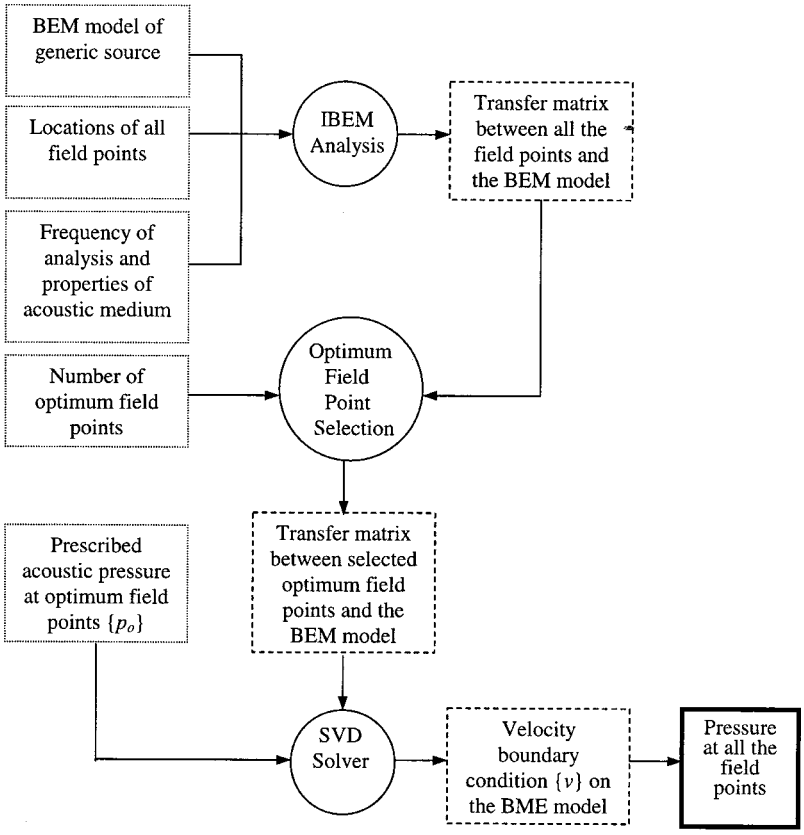

FIG. 1. Flow chart of the field reconstruction process.

shapes for both interior and exterior fields.[9,10] The HELS method is based on an expansion of spheroidal functions, and allows recovery of the pressure field on the surface of the noise sources.

In order to identify the best field points for collecting acoustic data for a source reconstruction computation the effective independence (EFI) method[11,12] was combined with the SVD algorithm and the direct boundary element method.[7,8] The optimal field point selection process identifies linearly independent measurement locations for source reconstruction based on measurements for both an interior[7] and an exterior acoustic field.[8] The EFI method bases the selection of points on the independence of the Fisher information matrix associated with an already orthogonal basis. Consequently the number of selected points has to be higher or equal to the number of vectors in the basis. Therefore, when the EFI was combined with the direct boundary element method for identifying the optimal field points, a requirement was imposed to the number of selected optimal field points to be higher than the number of elements where the velocity was computed.[7,8]

The work presented in this paper targets the computation of appropriate velocity boundary conditions on the surface of a generic source that has approximately the same dimensions with the actual source, in order to recreate the acoustic field that was originally generated by the actual source. Based on the IBEM formulation, transfer functions are defined between the acoustic response at field points, and the velocity boundary conditions on the generic source. A system of equations and a transformation matrix can be assembled from the transfer functions. The velocity boundary conditions on the generic source constitute the unknown variables. A SVD algorithm[13] is employed for solving the final system of equations formulated by the IBEM. An iterative algorithm that selects the optimum location of a prescribed number of points from a set of candidate points is developed. The capability to select the optimum points from a candidate set can be utilized for reducing the number of field points required in the field reconstruction computation. The number of optimum points can be considerably less than the number of elements where the velocity is computed. The flow chart of the developed field reconstruction process is demonstrated in Fig. 1. Several field reconstructions are performed in order to validate the development. The impact on the quality of the results of selecting field points in an optimal manner is demonstrated.

The new developments presented in this paper are: (i) A field reconstruction algorithm based on the IBEM (the IBEM is a substantially different boundary element formulation than the direct boundary element method that has been employed in previous source reconstruction developments). (ii) Development of an algorithm for the selection of optimal field points based on maximizing the quality of the reconstruction by optimizing the orthogonality property of the vectors that comprise the range of the transformation matrix. The number of optimal points is considered to be less than the number of elements where the velocity is computed.

II. MATHEMATICAL FORMULATION

A brief overview of the IBEM is presented first. A SVD algorithm employed for computing the element velocities that recreate the prescribed acoustic field is introduced. A

selection algorithm that identifies the optimum location of a prescribed number of field points from a set of candidate points is also presented.

A. Overview of indirect boundary element method

In the IBEM the primary variables of the formulation are defined as the difference in the pressure, and the difference in the normal gradient of the pressure between the two sides of a boundary element model.[14] The acoustic pressure at any data recovery point can be computed by the surface integral:

$$p(\mathbf{r})=\int_{S_Y}\left(G(\mathbf{r},\mathbf{r}_Y)\,\delta dp(\mathbf{r}_Y)-\frac{\partial G(\mathbf{r},\mathbf{r}_Y)}{\partial \hat{n}_Y}\,\delta p(\mathbf{r}_Y)\right)dS_Y, \tag{1}$$

where S_Y=surface of the boundary element model, subscript ''Y'' indicates a source point on the boundary element surface, $\mathbf{r}$=position vector for the field point, $p(\mathbf{r})$=acoustic pressure at a point defined by position vector $\mathbf{r}$, $\mathbf{r}_Y$=position vector of a source point on the surface of the model, $\hat{n}_Y$=unit normal at the location of the source point, the Green's function, $G(\mathbf{r},\mathbf{r}_Y)$ is defined as $G(\mathbf{r},\mathbf{r}_Y)=(1/4\pi|\mathbf{r}-\mathbf{r}_Y|)\times e^{-j|\mathbf{r}-\mathbf{r}_Y|}$, $\delta dp(\mathbf{r}_Y)$, $\delta p(\mathbf{r}_Y)$=primary variables of the IBEM defined as the difference in the normal gradient of the pressure and the difference in the pressure, respectively, between the two sides of the boundary element model.[14] The difference in the normal gradient of the pressure can be defined

$$\begin{aligned}\delta dp(\mathbf{r}_Y)&=\frac{\partial p(\mathbf{r}_{Y_1})}{\partial \hat{n}_Y}-\frac{\partial p(\mathbf{r}_{Y_2})}{\partial \hat{n}_Y}\\&=-j\rho\omega(v(\mathbf{r}_{Y_1})+v(\mathbf{r}_{Y_2})),\end{aligned} \tag{2}$$

where subscripts ''1'' and ''2'' are associated with the two sides of the boundary element model, ρ=density of the acoustic medium, ω=radial frequency, $v(\mathbf{r}_{Y_1})$=acoustic velocity on side ''1'' of the model at location $\mathbf{r}_Y$, and $v(\mathbf{r}_{Y2})$=acoustic velocity on side ''2'' of the model at location $\mathbf{r}_Y$. The difference in the acoustic pressure across the surface of the boundary element model can be defined

$$\delta p(\mathbf{r}_Y)=(p(\mathbf{r}_{Y_1})-p(\mathbf{r}_{Y_2})). \tag{3}$$

The definition of the primary variables contains information for the acoustic spaces from both sides of the model. Thus, the IBEM can model a thin source that radiates from both sides and can account for openings in the acoustic model. The definition of the primary variables and the assembly of the primary system of equations constitute major differences between the direct and indirect methods.

By considering for simplicity a structural velocity boundary condition over the entire boundary element model (general boundary conditions such as pressure, velocity and unequal impedance are possible[14–16]) the boundary condition becomes

$$v(\mathbf{r}_{X_1})=-v(\mathbf{r}_{X_2})=\overline{v}(\mathbf{r}_X)\Rightarrow\delta dp(\mathbf{r}_X)=0 \quad \text{on} \quad S_v\equiv S_Y, \tag{4}$$

where $\overline{v}(\mathbf{r}_X)$=structural velocity at a location of the boundary element model defined by the point vector $\mathbf{r}_X$, S_Y=surface of the entire boundary element model, and S_v=surface with velocity boundary condition. An integral form of the boundary condition can be created by differentiating Eq. (1), taking into account the relationship between the normal gradient of the pressure and the acoustic velocity, and combining them with Eq. (4),

$$\begin{aligned}-j\rho\omega\overline{v}(\mathbf{r}_X)&=\frac{\partial p(\mathbf{r}_X)}{\partial \hat{n}_X}\\&=\int_{S_Y}\left(-\frac{\partial^2 G(\mathbf{r}_X,\mathbf{r}_Y)}{\partial \hat{n}_X\partial \hat{n}_Y}\,\delta p(\mathbf{r}_Y)\right)dS_Y.\end{aligned} \tag{5}$$

A numerical solution is obtained through the variational principle[17] stating that the solution to the equation,

$$f=\Re(\phi), \tag{6}$$

will also minimize the functional[17]

$$F(\phi)=\int_S \phi\Re(\phi)dS-2\int_S \phi f dS, \tag{7}$$

where $\Re(\phi)$=the operator on function ϕ, f=a known function, and $F(\phi)$=the quadratic functional. By identifying the correspondence between the terms of Eq. (5) and the terms of Eq. (6) a functional can be generated according to Eq. (7),

$$\begin{aligned}F_v=2\int_{S_X} j\rho\omega\overline{v}(\mathbf{r}_X)\,\delta p(\mathbf{r}_X)dS_X-\int_{S_X}\delta p(\mathbf{r}_X)\\\times\left(\int_{S_Y}\left(\frac{\partial^2 G(\mathbf{r}_X,\mathbf{r}_Y)}{\partial \hat{n}_X\partial \hat{n}_Y}\,\delta p(\mathbf{r}_Y)\right)dS_Y\right)dS_X.\end{aligned} \tag{8}$$

By imposing a stationarity condition on F_v with respect to the unknown primary variables $\delta p(\mathbf{r}_X)$ results in a linear system of equations that allows computation of $\delta p(\mathbf{r}_Y)$ over the entire boundary element model.

The unknown functions of the primary variables on the surface of the boundary element model are expressed in terms of the unknown nodal values of the primary variables at the nodes of the boundary element model, and the element shape functions as

$$\delta p(\mathbf{r}_X)=\{N_i\}^T\{\delta p_i\}, \tag{9}$$

where $\{\delta p_i\}$=column vectors of nodal values of the primary variables at the nodes of the ith element, and $\{N_i\}$=column vector of the shape functions associated with the ith element. Spatial derivatives of the primary variables can be also expressed in terms of the nodal values of the primary variables and the spatial derivatives of the shape functions. The final numerical system of equations is derived by imposing a stationarity condition on F_v with respect to the unknown primary variables. It leads to a system of equations

$$[A]\{q\}=\{f\}, \tag{10}$$

where $[A]$=the acoustic system matrix, $\{q\}$=vector of unknown primary variables on the surface of the BEM model, and $\{f\}$=vector representing the excitation, derived from the velocity boundary condition. The system matrix $[A]$ is square

and symmetric since it is derived by a variational formulation. The terms of matrix $[A]$ are generated from the numerical formulation and the stationarity condition associated with the second integral of Eq. (8). The terms of the excitation vector $\{f\}$ are generated from the first integral of Eq. (8).

B. Formulation of the inverse analysis

Once the distribution of the primary variables is computed by Eq. (10), the integral defined in Eq. (1) can be employed to compute the acoustic response at any field point. By taking into account the numerical discretization introduced by Eq. (9), the computations associated with recovering the acoustic pressure at several field points can be written in matrix form

$$\overbrace{\{p_o\}}^{M\times 1}=\overbrace{[DR]}^{M\times N}\overbrace{\{q\}}^{N\times 1}, \tag{11}$$

where $\{p_o\}$=vector of acoustic pressure at ''M'' number of field points, $[DR]$=matrix with entries derived from the integrals of Eq. (1), and ''N''=number of nodal primary variables present in the boundary element formulation. According to Eq. (10) $\{q\}$ can be expressed in terms of $[A]$ and $\{f\}$. Then,

$$\overbrace{\{p_o\}}^{M\times 1}=\overbrace{[DR]}^{M\times N}\overbrace{[A]^{-1}}^{N\times N}\overbrace{\{f\}}^{N\times 1}. \tag{12}$$

The vector $\{f\}$ is generated from the integral $2\int_{S_X} j\rho\omega\overline{v}(\mathbf{r}_x)\delta p(\mathbf{r}_x)dS_X$ of Eq. (8). The integral, and therefore the terms of vector $\{f\}$, are linear functions of the velocity boundary conditions $\overline{v}(\mathbf{r}_X)$. Thus, the vector $\{f\}$ can be expressed as a product between a matrix and the vector of velocity boundary conditions,

$$\overbrace{\{f\}}^{N\times 1}=\overbrace{[FV]}^{N\times K}\overbrace{\{\overline{v}\}}^{K\times 1}, \tag{13}$$

where $\{\overline{v}\}$=vector of velocity boundary conditions applied on the elements of the boundary element model, and ''K'' =number of elements in the boundary element model. The entries of $[FV]$ are derived from integrals of the form

$$\int_{S_X} j\rho\omega\{N_i\}\{N_j\}^T dS_X \rightarrow [FV]. \tag{14}$$

Introducing Eq. (13) into Eq. (12) results in

$$\overbrace{\{p_o\}}^{M\times 1}=\underbrace{\overbrace{[DR]}^{M\times N}\overbrace{[A]^{-1}}^{N\times N}\overbrace{[FV]}^{N\times K}}_{\underbrace{[B]}_{M\times K}}\overbrace{\{\overline{v}\}}^{K\times 1}\Rightarrow\overbrace{\{p_o\}}^{M\times 1}=\overbrace{[B]}^{M\times K}\overbrace{\{\overline{v}\}}^{K\times 1}. \tag{15}$$

The transformation matrix $[B]$ establishes a direct relationship between the velocity boundary conditions on the surface of the generic source and the acoustic pressure at the field points. Equation (15) is employed for computing the velocity on the surface of a generic source in order to recreate a prescribed acoustic field. For practical reasons it is beneficial to utilize the least possible number of field points for collecting information for the acoustic field. Therefore, in the work presented in this paper the number of field points ''M'' is always considered to be less than the number of elements ''K'' where velocities are being computed. The SVD algorithm and the optimum point selection algorithm have been developed based on the expectation that $M<K$. Matrix $[B]$ contains the following information:

(i) frequency of analysis and the fluid properties (ρ,c,ω),
(ii) relative position between the field points and the boundary element model (matrix $[DR]$),
(iii) complex geometry of the source (boundary element matrices $[DR]$, $[A]$),
(iv) contribution of each element to the excitation applied on the acoustic system (matrix $[FV]$).

In the field reconstruction process the information about the acoustic response $\{p_o\}$ originating from the actual source is considered to be prescribed. The velocity boundary conditions $\{\overline{v_o}\}$ that can be applied on a generic source are computed by employing a SVD solution algorithm[13] for solving Eq. (15). It is necessary to employ a SVD algorithm because $[B]$ is not a square matrix and therefore $[B]^{-1}$ does not exist. Since in this paper it is considered that $M<K$, the solution $\{\overline{v_o}\}$ to Eq. (14) is not unique because any linear combination of vectors from the null space can be added to the solution. However, out of all the possible solutions the one selected as final is the solution that exhibits the smallest magnitude $|\{\overline{v_o}\}|$.[13] According to SVD algebra the $M\times K$ matrix $[B]$ can be written as[13]

$$\overbrace{[B]}^{M\times K}=\overbrace{[U]}^{M\times K}\overbrace{[W]}^{K\times K}\overbrace{[V]^T}^{K\times K}, \tag{16}$$

where $[U]$=a $M\times K$ column matrix, $[W]$=a $K\times K$ diagonal matrix with positive or zero diagonal entries, and $[V]^T$=the transverse of a $K\times K$ orthogonal matrix $[V]$. The columns of $[U]$ that correspond to nonzero diagonal entries of $[W]$ are expected to constitute an orthogonal set of basis vectors that span the range of matrix $[B]$. The columns of $[V]$ that correspond to the zero diagonal terms of $[W]$ constitute an orthogonal basis for the null space. Thus, vectors can be appropriately designated to belong either to the basis of the range of the transformation or to the null space depending on the value of the diagonal terms of matrix $[W]$. The selection of the solution that exhibits the lowest magnitude is made by appropriately assigning in the null space the vectors associated with small diagonal entries in matrix $[W]$. Due to the expected orthogonality properties the basis of the transformation and the basis of the null space are considered to satisfy the equation

$$\overbrace{[U]^T}^{K\times M}\overbrace{[U]}^{M\times K}=\overbrace{[I]}^{K\times K}=[V]^T[V]=[V][V]^T. \tag{17}$$

Once $[U]$, $[W]$, and $[V]$ have been computed by the SVD then Eq. (15) can be employed to calculate $\{\overline{v_o}\}$,

$$[B]\{\bar{v}_o\}=\{p_o\}\Rightarrow[U][W][V]^T\{\bar{v}_o\}=\{p_o\}$$
$$\Rightarrow[V][W]^+[U]^T[U][W][V]^T\{\bar{v}_o\}$$
$$=[V][W]^+[U]^T\{p_o\}$$
$$\Rightarrow\{\bar{v}_o\}=[V][W]^+[U]^T\{p_o\}, \quad (18)$$

where $[W]^+$ is the Moore-Penrose pseudoinverse of $[W]$.[18] In this manner there is no need to invert the nonsquare matrix $[B]$ because $[B]^{-1}$ does not exist. Instead, the decomposition of $[B]$ into the basis of the range and the basis of the null space are utilized for solving the underdetermined system of equations. An important aspect of the SVD algorithm is associated with the replacement of the small diagonal terms of matrix $[W]$ with zero entries. The replacement process determines whether to consider the corresponding vector as a component of the basis associated with either the range $[U]$ or the null space $[V]$ of the transformation matrix $[B]$. Vectors of the range $[U]$ correspond to nonzero diagonal entries and vectors of the null space correspond to zero diagonal entries. The diagonal terms of $[W]^+$ that correspond to the zero entries of $[W]$ are also replaced by a zero entry. This last substitution results in obtaining, out of all possible solutions, the one with the smallest length when $M<K$.[13]

C. Selection of optimum field points for the field reconstruction

In previous work the EFI method[11,12] was combined with the direct BEM for selecting the best field points of an interior[7] or an exterior[8] acoustic field in order to collect data for reconstructing the source. The EFI method was originally developed for placing sensors on space structures for modal identification on orbit.[11,12] The EFI formulation originates from requiring the modal degrees of freedom computed by a finite element analysis to be equal to the modal degrees of freedom identified by the sensors. The number of sensors is always considered to be at the very least, equal to the number of modal degrees of freedom that will be retrieved. Thus, the EFI algorithm deletes redundant information by eliminating sensor locations that do not contribute significantly to the independent information contained within the target mode partitions. The sensors that are eliminated are identified by generating the Fisher information matrix from the already orthogonal modal matrix. The absolute identification space is computed by evaluating the eigenvalues and eigenvectors of the Fisher information matrix. The original orthogonal modal matrix and the basis vectors of the absolute identification space are utilized for calculating the fractional contribution of each sensor location to each eigenvector of the absolute identification space. Based on the fractional contribution of each sensor it is determined which sensors offer the highest independent information to the already orthogonal modal matrix. Since the EFI formulation is structured to identify independent information from an already orthogonal modal matrix, it cannot accommodate identification of a smaller number of optimum sensor locations than the number of modes contained in the original orthogonal matrix. The implementation of the EFI method to the source reconstruction processes for interior[7] or exterior[8] acoustic fields imposes a similar requirement on identifying a larger number of optimum field points than number of elements where the velocity is reconstructed.

In this work an alternative iterative formulation is developed in order to identify optimal field points for collecting acoustic pressure data. The number of optimal field points is considered smaller than the number of elements where velocities are computed. Instead of using the independence of the information in an already orthogonal matrix as a selection criterion, the developed algorithm is based on selecting field points that maximize the quality of the reconstruction. The fidelity of the reconstructed field is high when the orthogonality demonstrated by the range of the transformation matrix is high. The location of the field points impacts the selection of the vectors that constitute the basis of the range of the transformation matrix. Therefore, achieving the highest possible orthogonality is utilized as criterion for selecting the optimal field points. The new algorithm can be utilized when the number of the optimum field points is lower than the number of elements where the velocity is computed.

The starting point for the optimum field point selection algorithm is the requirement for the reconstructed field pressure to be the same with the baseline field pressure. The acoustic pressure for the recreated field can be evaluated by combining Eq. (15) and Eq. (18),

$$\{p_r\}=[B]\{\bar{v}_o\}=[B][V][W]^+[U]^T\{p_o\}$$
$$=[U][W]\underbrace{[V]^T[V]}_{[I]}[W]^+[U]^T\{p_o\}$$
$$=\underbrace{[U]}_{M\times K}\underbrace{[W]}_{K\times K}\underbrace{[W]^+}_{K\times K}\underbrace{[U]^T}_{K\times M}\{p_o\}, \quad (19)$$

where $\{p_r\}$=vector of reconstructed acoustic pressure from the generic source. Since M is less than K, in order to obtain out of all possible selections the one with the smallest length, the small diagonal terms of $[W]$ and the equivalent positions of $[W]^+$ are replaced by zero terms. In this manner the product of $[W]$ and $[W]^+$ is not equal to the identity matrix, but equal to a $K\times K$ matrix that has unit entries at the diagonal locations that correspond to the vectors of the range of the transformation and zero entries everywhere else. Therefore, the product,

$$\underbrace{[T]}_{M\times M}=\underbrace{[U]}_{M\times K}(\underbrace{[W][W]^+}_{K\times K})\underbrace{[U]^T}_{K\times M}, \quad (20)$$

constitutes a transfer matrix between the original and the reconstructed fields. The right-hand side of Eq. (20) depends on the orthogonality property demonstrated by the basis of the range of the transformation. Therefore, when the orthogonality property is high $[T]$ tends to be equal to the identity matrix and the acoustic field is reconstructed accurately. Each diagonal entry of matrix $[T]$ is related to a particular field point. The selection of the location of the field points influences the derivation of the range and the orthogonality property demonstrated by its basis vectors. An iterative process is established for selecting the optimum location for a prescribed number of field points from a set of candidate points in order to maximize the orthogonality property

of the range of the transformation. Within each iteration matrix $[T]$ is computed, and the field point that corresponds to the lowest diagonal value is eliminated from the set of candidate points. For the remaining points matrices $[U]$, $[W]$, and $[V]$ are evaluated again, and the product $[T]$ is computed. With each iteration the criterion of the smallest resulting velocity vector is utilized in order to determine whether a vector will be assigned to the basis of the range or the basis of the null space of the transformation matrix. The elimination process continues until the number of the remaining field points is equal to the number of points requested to be identified by the optimum search process. The developed optimum search process can also be utilized to identify the best field points over a frequency range. An extra inner loop over the frequency range is added to the iteration process. The elimination of the field points is based on the lowest sum of magnitudes of the diagonal terms over a frequency range rather than at a single frequency. The identification of the optimum locations for the field points is strictly a function of the geometry of the generic source, the frequency of analysis, the acoustic medium, and the relative position of the candidate field points with respect to the source. The selection of optimum field points does not depend on the actual pressure values of the original field, since $\{p_o\}$ does not enter into the computations associated with the derivation of $[U]$, $[W]$, and $[V]$.

III. VALIDATION / APPLICATION

The field reconstruction capability presented in this paper and the optimum field point selection algorithm are validated extensively. Four different types of acoustic fields derived from analytical solutions are utilized in the validation for creating the baseline field information. Velocity boundary conditions are computed on generic sources in order to recreate the baseline fields. A pulsating line source of finite length and a vibrating piston set in a rigid sphere are two examples utilized in the past for validating a source reconstruction development[6] and they are also employed in this paper. In addition, the analytical solution of a quadrupole and the analytical solution of an array of point sources positioned in a plane are utilized for demonstrating the new computational capabilities. The unique capability of the IBEM to capture radiation from both sides of a boundary element model allows definition of thin planar surfaces as generic sources. Appropriate velocity boundary conditions are computed through the developed process. For all four types of acoustic fields a considerably smaller number of field points than number of elements in the boundary element model are utilized in the reconstruction. The field points are identified by the optimal field point selection algorithm presented in this paper. Results for the reconstructed field based on the optimally selected points are compared to the baseline solution and to reconstruction results based on an equal number of evenly distributed field points. The baseline and the reconstructed fields are computed at a larger number of field points than the ones actually used in the reconstruction. Therefore, the correlation is inspected for the overall radiated field and at points that do not participate in the reconstruction process. A metric based on the radiated acoustic power is used in order to compare the solutions. In addition, the radiation patterns and the sound pressure levels are also compared during the validation.

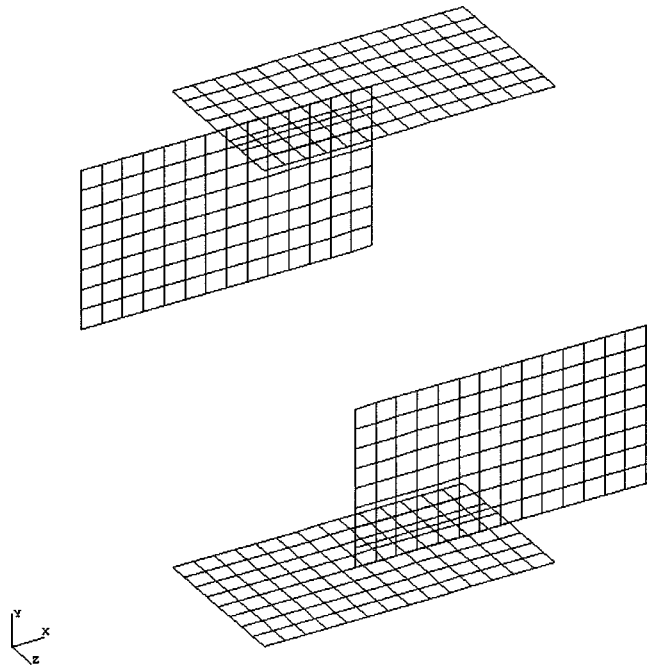

FIG. 2. Boundary element model of the generic source utilized to reconstruct the field generated by a line source.

A. Reconstruction of acoustic field originating from line source

The acoustic field generated by a line source of finite length is considered in this analysis. The line source has length equal to 0.5 m, radius equal to 0.01 m, and radial velocity equal to 100 m/sec. The parameters for the line source are identical to the values utilized in Ref. 6. In order to demonstrate the unique capabilities that the IBEM provides in the field reconstruction process the generic source is considered to be composed of four planes with dimensions 0.6×1.1 m each. Each plane comprises 112 elements that radiate noise from both sides. The four planes are positioned at 0.6 m apart and the boundary element model is depicted in Fig. 2. Since the generic source does not contain an enclosed acoustic cavity there are no irregular frequencies present in the analysis. The capability to model thin sources that radiate noise from both sides is unique to the IBEM and to the field reconstruction technique presented in this paper. The field surface is a sphere with radius equal to 3.0 m and center at the middle of the line source. It is comprised of 98 field points. Reconstruction analyses are performed at $ka=2$ and $ka=4$ similar to Ref. 6 as well as $ka=0.5$, $ka=1$, and $ka=3$. Thirty field points are selected optimally by the developed algorithm for $ka=0.5$, $ka=1$, and $ka=2$ while 50 field points are selected optimally for $ka=3$ and $ka=4$. Values of the original acoustic field at the optimally selected field points are employed to reconstruct the velocity boundary conditions on the generic source. The acoustic field is reconstructed and results are computed at all 98 field points. In order to demonstrate the importance of selecting the field points in an optimal manner the field reconstruction compu-

TABLE I. Radiated acoustic power for continuous line source.

ka	Original (watts)	Optimal (watts)	Error (%)	Even (watts)	Error (%)
0.5	924.75	920.36	0.47	891.34	3.61
1	3069.7	3003.6	2.15	3356.2	9.33
2	6519.7	6378.5	2.17	7008.0	7.49
3	9394.4	9241.5	1.63	8003.5	14.8
4	14 490	14 326	1.13	11 683	19.4

tations are repeated based on acoustic data collected at an equal number of evenly distributed field points. The radiated acoustic power is computed from acoustic pressure and acoustic velocity data calculated at all 98 field points and the results are summarized in Table I. It can be observed that when the optimally selected points are utilized in the computations the maximum error encountered in the radiated power is 2.17%, while for an equal amount of evenly distributed points the maximum error is 19.4%. These results demonstrate that achieving the highest possible orthogonality in the basis of the range of the transformation matrix impacts significantly the quality of the reconstructed field. The developed algorithm for the optimal point selection is based on maximizing the orthogonality property. Therefore, there is significant difference in the results between optimally selected and evenly selected field points.

B. Reconstruction of acoustic field originating from a vibrating piston set in a rigid sphere

A sophisticated source utilized by Ref. 6 is also employed in this paper to further validate and demonstrate the new developments. A vibrating piston is set in the side of a rigid sphere with radius equal to 0.2 m. The spherical piston surface spans an angle of 30°. The piston velocity is defined equal to 1 m/sec. The field pattern and the directivity depend on the Helmholtz number ka. Analyses are performed at $ka=2$ and $ka=4$. The properties of the source and the frequencies of analysis are identical with the values utilized in Ref. 6. The generic source is comprised in this case by a cube with dimension equal to 0.4 m. The center of the cube is the same with the center of the sphere. The boundary element model comprises 150 elements and 152 nodes. A spherical field surface composed of 98 points is defined with

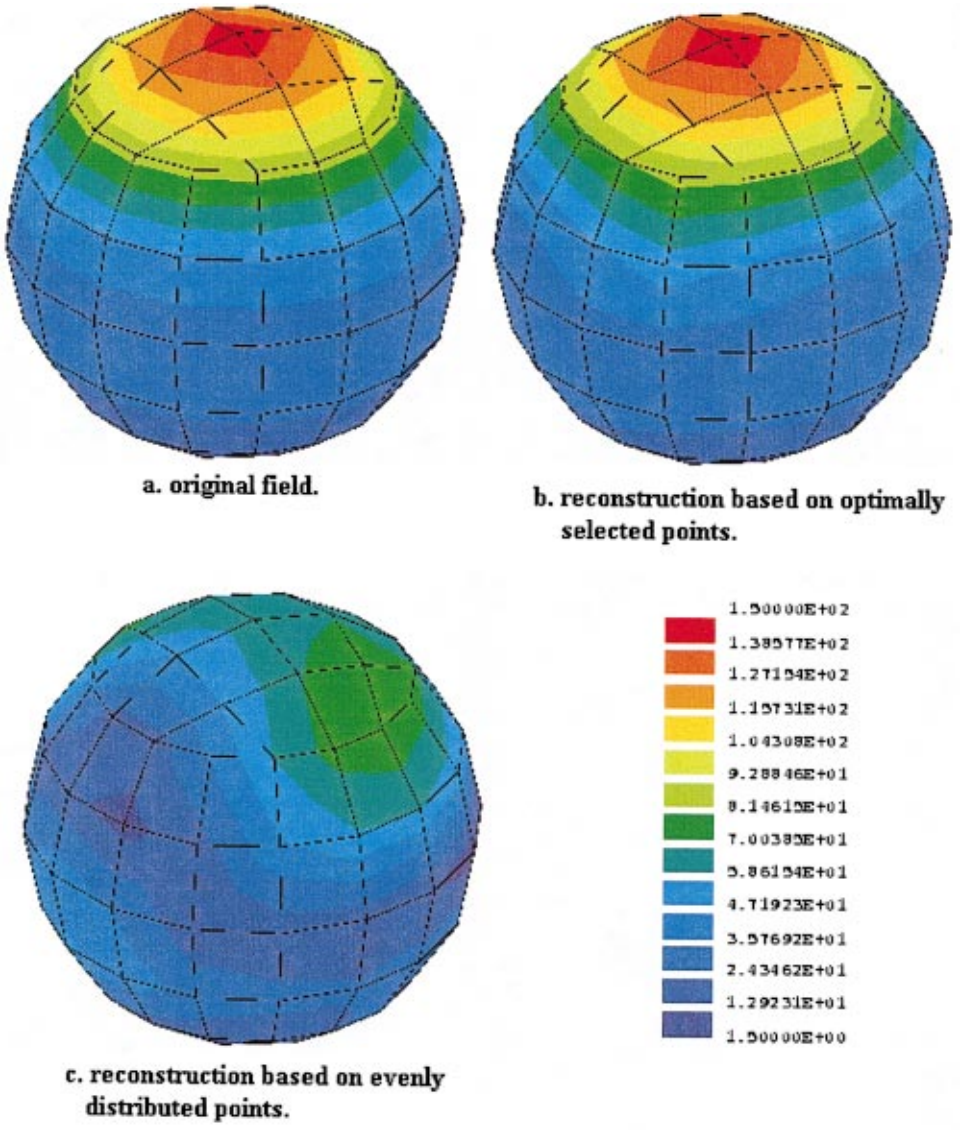

FIG. 3. Magnitude of acoustic pressure of original and reconstructed field; vibrating piston in a sphere; $ka=2$.

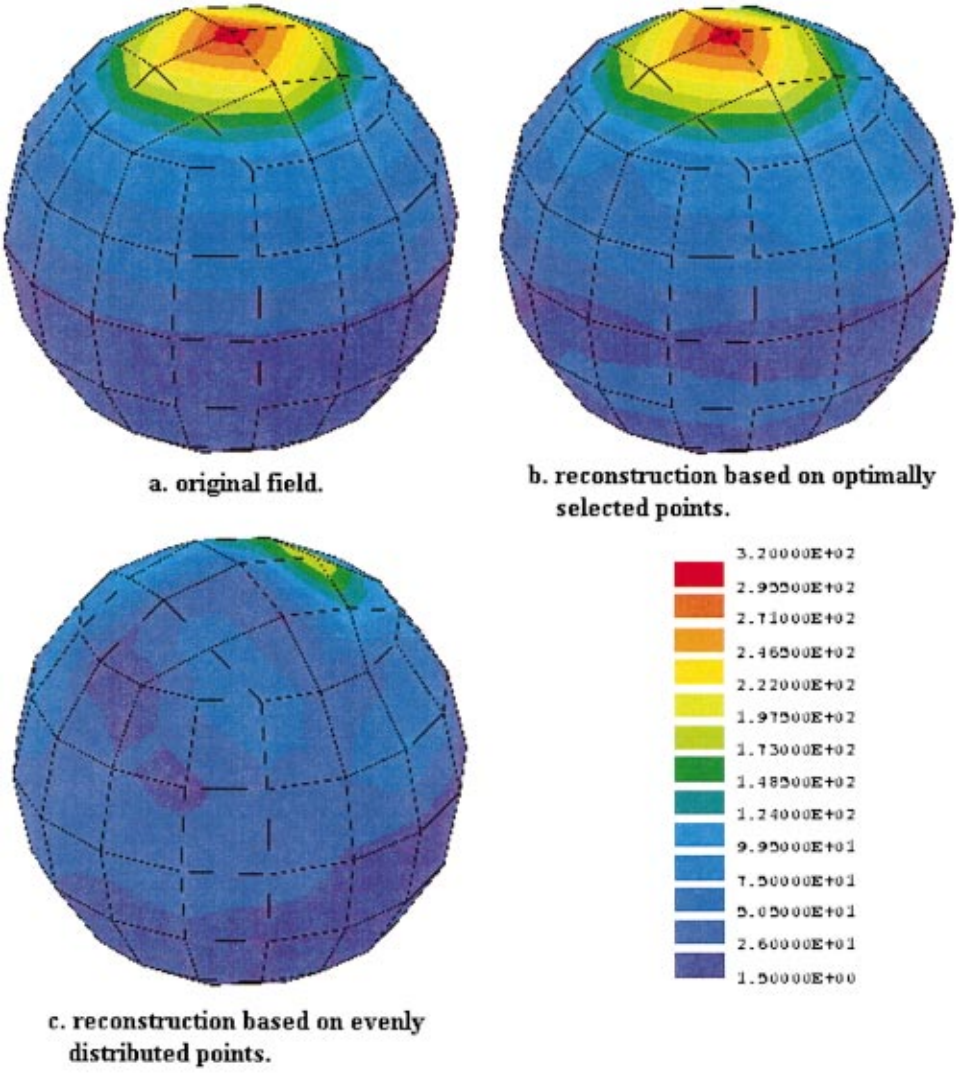

FIG. 4. Magnitude of acoustic pressure of original and reconstructed field; vibrating piston in a sphere; $ka=4$.

0.4 m radius and a center coinciding with the center of the rigid sphere and the cube. The field reconstructions for $ka=1$ are performed based on field data collected at 30 optimally selected and evenly distributed points. The computations $ka=4$ are based on field information collected at 45 field points. In both cases the number of field points is considerably smaller than the number of elements in the boundary element model. The optimal field points are selected from the original 98 points that comprise the field surface. Results for the acoustic pressure at all 98 field points and for Helmholtz numbers $ka=2$ and $ka=4$ are presented in Figs. 3 and 4, respectively. In each figure the magnitude of the acoustic pressure from the baseline field and the two reconstructed fields are presented. The same color scale is employed for all the results in each figure. As expected, the field reconstructed from acoustic data collected at the optimally selected field points produces accurate results for both Helmholtz numbers. The generic source recreates the acoustic field well both at the optimally selected field points that are utilized in the computations, and at field points where the acoustic pressure is not considered during the reconstruction process. The quality of the results computed from acoustic data collected at evenly distributed points is inferior in terms of both the magnitude and the radiation pattern of the reconstructed field. Therefore, the importance of selecting the field points in an optimal manner that achieves the highest possible orthogonality for the range of the transformation matrix is demonstrated.

C. Reconstruction of acoustic field originating from quadrupole

A quadrupole source is utilized to create a baseline acoustic field at 100, 300, 500, 700, and 1000 Hz, respectively. The spacing between two adjacent point sources is 0.01 m. Each one of the four point sources has unit strength and is 180° out of phase with adjacent source. A boundary element model of a box with dimensions $0.2\times0.2\times0.2$ m is comprised of 24 elements, and it is employed as a generic source in the analysis. A spherical field surface of 1 m radius composed of 98 field points is defined. Nine optimally selected and nine evenly distributed points are utilized in two separate reconstruction computations. Figure 5 depicts the two sets of points on the data recovery surface. The magnitude of the acoustic pressure of the baseline acoustic field and the two reconstructed fields based on optimally selected and evenly distributed field points are presented in Fig. 6 for 500 Hz. When the optimally selected field points are em-

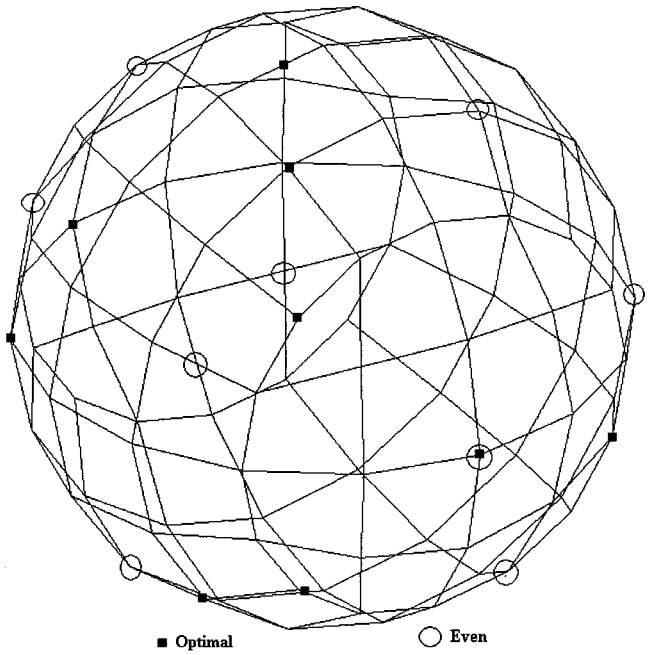

FIG. 5. Distribution of the optimally selected and evenly distributed field points utilized for reconstructing a field created by a quadrupole.

ployed in the reconstruction, the results are identical with the analytical solution for all 98 points (although only 9 points are employed in the reconstruction). For the evenly selected points the results deteriorate. The difference in the reconstructed results originates from the transfer matrix $[T]$ [Eq. (20)] that relates the original and the reconstructed fields. When the range of the transformation matrix $[B]$ comprises an orthogonal set of vectors, then the transfer matrix $[T]$ is expected to be equal to the identity matrix. For the optimally selected points $[T]$ is in fact equal to the identity matrix. For the evenly distributed points the diagonal entries of $[T]$ range from 0.7 to 1.0, and the nonzero off-diagonal terms range between -0.3 and 0.3. The capability to optimally select points is important when it is desired to limit the total number of field points employed in the reconstruction. The situation is similar for the field reconstruction at all other frequencies. Results for the radiated power computed on the spherical field surface are summarized in Table II. Results for the baseline and the reconstructed fields based on the even and optimal distribution of field points are presented. The maximum error encountered in the results from the op-

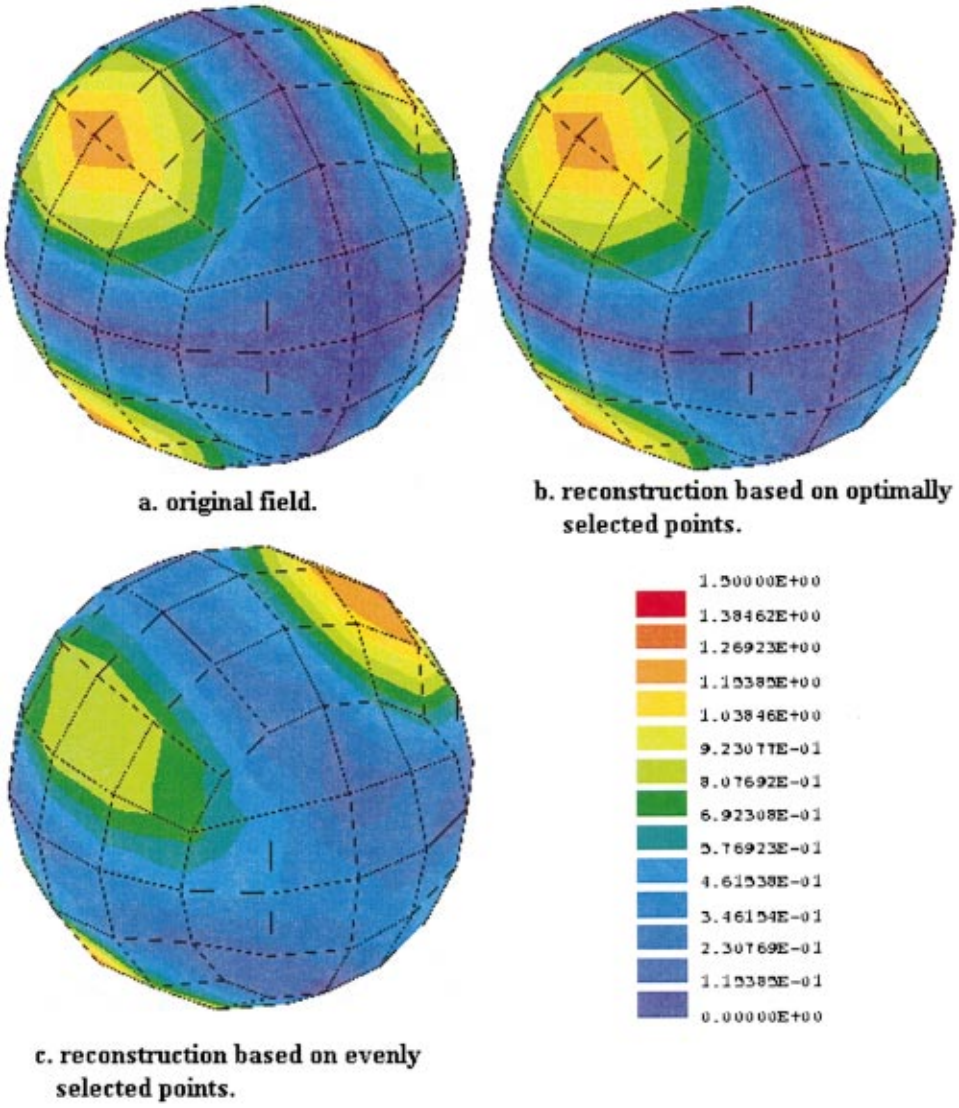

FIG. 6. Magnitude of acoustic pressure of original and reconstructed field; quadrupole field; 500 Hz.

TABLE II. Radiated acoustic power for quadrupole source.

Frequency (Hz)	Original (watts)	Optimal (watts)	Error (%)	Even (watts)	Error (%)
100	3.811E-7	3.816E-7	0.118	3.756E-7	1.44
300	2.782E-4	2.775E-4	0.252	2.933E-4	5.43
500	0.005 962	0.005 993	0.520	0.005 597	6.12
700	0.044 86	0.044 62	0.535	0.045 87	2.25
1000	0.3809	0.3842	0.866	0.3721	2.31

timally distributed points is 0.87%, while the maximum error encountered in the results from the evenly distributed points is 6.12%.

D. Reconstruction of acoustic field originating from a planar distribution of multiple point sources

An acoustic field generated by multiple point sources positioned on a plane is employed in this analysis. The point sources are equally spaced on a plane with dimensions 0.2 by 0.4 m. The spacing between two adjacent point sources is 0.02 m. Each point source has unit strength. The phase of adjacent sources varies by 180°. A spherical field point surface with 0.6 m radius and center positioned at the center of the plane with the sources is defined. The field surface is composed of 98 points. The generic source is defined by two perpendicular planes (Fig. 7). The length of the planes is equal to 0.4 m and the width is equal to 0.2 m. Noise is radiated from both sides of the two planes. Multiple connection and free edge conditions are present in the boundary element model. Field reconstruction analyses are performed at 100, 300, 500, 700, and 1000 Hz, respectively. The reconstructions are based on field data collected at 60 optimally and evenly selected points. All the points of the field surface are considered as candidate points. The optimal points are selected based on a multifrequency criterion. The even and the optimal distributions of field points are presented in Fig. 8. Results for the radiated sound power of the original field and the reconstructed fields are summarized in Table III. The maximum error in the sound power computation for the reconstruction based on optimally distributed points is 4.3%, while the maximum error for the reconstruction based on evenly distributed points is 22%. The sound pressure level

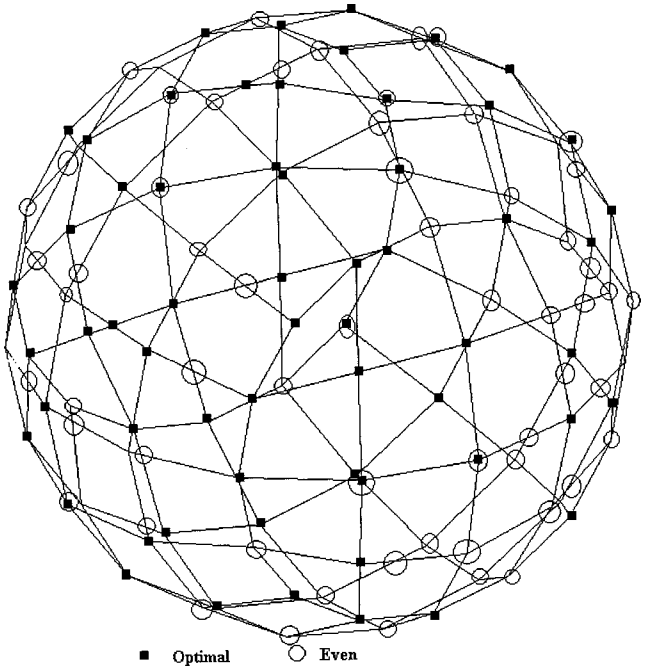

FIG. 8. Evenly and optimally distributed field points utilized to reconstruct the field generated by multiple point sources on a plane.

from the original field and the two reconstructed fields are presented in Fig. 9 for 1000 Hz. Similar to the previous applications it can be observed that the field reconstruction based on the optimally selected points produces considerably more accurate results than the field reconstruction based on an equal amount of evenly distributed points. The results for both the magnitude of the sound power level and the radiation pattern are inaccurate when the evenly distributed field points are employed in the reconstruction. The results improve dramatically when the same number of field points is optimally distributed. In this application the generic source is comprised from thin surfaces that radiate from both sides. Therefore, no irregular frequencies will appear in the analysis and the field reconstruction computations.

IV. CONCLUSIONS

A field reconstruction process is presented in this paper. Velocity boundary conditions are computed on a generic

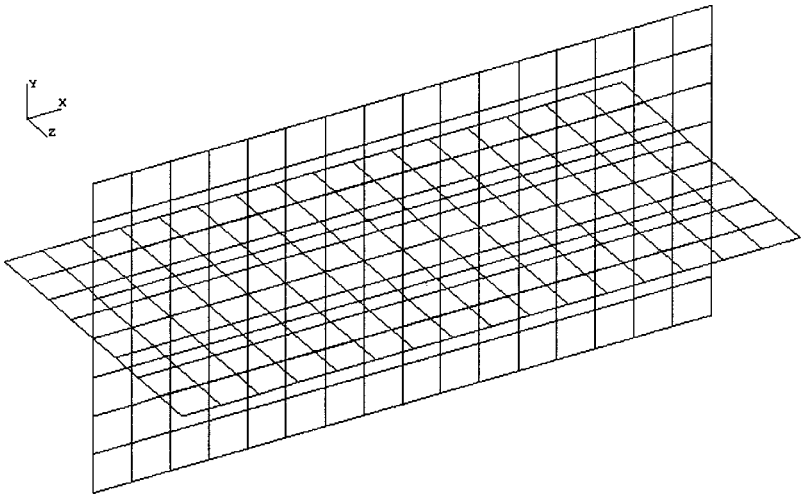

FIG. 7. Boundary element model of generic source utilized to reconstruct the field generated by multiple point sources on a plane.

TABLE III. Radiated acoustic power for multiple point sources in plane.

Frequency (Hz)	Original (watts)	Optimal (watts)	Error (%)	Even (watts)	Error (%)
100	0.1616	0.1553	3.90	0.1334	17.5
300	53.808	56.131	4.32	61.234	13.8
500	700.38	678.21	3.17	592.03	15.5
700	2685.3	2584.5	3.75	2231.4	16.9
1000	6353.7	6153.2	3.16	4930.3	22.4

source in order to recreate a prescribed acoustic field. The development is based on computing transfer functions between velocity boundary conditions on the surface of the generic source and the field points where the baseline field is defined. The computation of the transformation matrix is based on the IBEM. The IBEM offers the significant and unique capabilities of capturing radiation from both sides of a thin surface and including openings and multiple connections in the model. Using a thin open surface as a generic source eliminates the presence of irregular frequencies from the boundary element computations. A SVD algorithm is employed for computing the boundary conditions on the generic source and reconstructing the field. The original field is considered to be prescribed at a limited number of field points that is smaller than the number of elements in the boundary element model. Since an underdetermined system of equations must be solved, from all possible solutions the one that demonstrates the smallest magnitude is selected. It is demonstrated that the quality of the reconstructed field depends on the orthogonality exhibited by the range of the transformation matrix. The locations of the field points where the acoustic pressure of the baseline field is defined determines the orthogonality property of the range of the transformation matrix. An algorithm is developed that identifies the optimal locations of a prescribed number of field points from a set of candidate points. The selection algorithm is based on achieving the highest possible orthogonality for the basis of the range of the transformation matrix. The developments are validated by reconstructing the acoustic field generated from four different types of sources. The radiated sound power, the radiation pattern, and the sound pressure level of the radiated noise constitute metrics for the correlation. Good agreement is observed between the baseline field and the field reconstructed from acoustic data collected at optimally selected field points. The significance of field

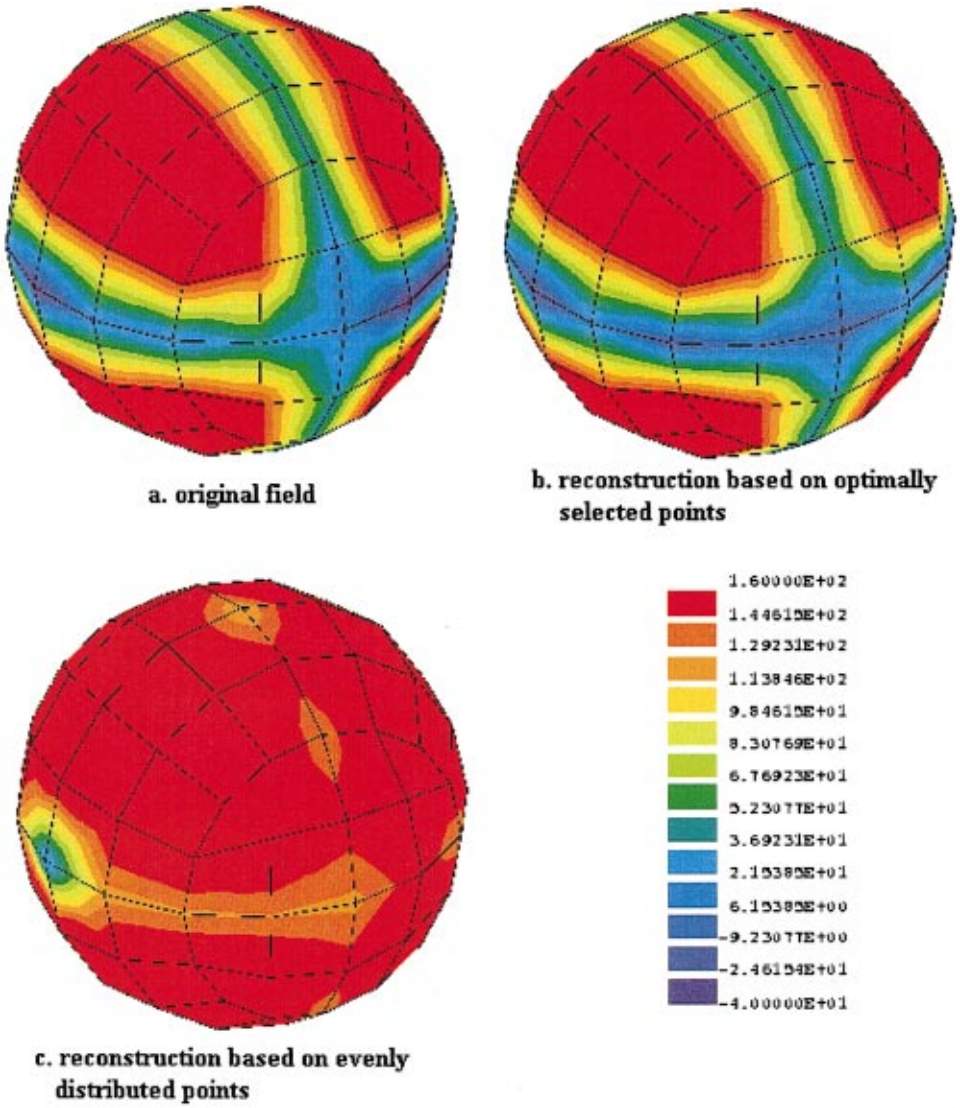

FIG. 9. Sound pressure level of original and reconstructed field; planar distribution of multiple point sources; 1000 Hz.

points selection on the quality of the results is demonstrated by comparing fields reconstructed from acoustic data collected at the same number of evenly and optimally distributed field points. The results computed from acoustic data collected at the optimal field points exhibit consistently high correlation with the baseline field.

ACKNOWLEDGMENTS

The work presented in this paper was funded by the Ford Motor Company University Research Program.

[1] J. D. Maynard, E. G. Williams, and Y. Lee, ''Nearfield acoustic holography: I. Theory of generalized holography and the development of NAH,'' J. Acoust. Soc. Am. **78**, 1395–1413 (1985).
[2] W. A. Veronesi and J. D. Maynard, ''Nearfield acoustic holography (NAH): II. Holographic reconstruction algorithms and computer implementation,'' J. Acoust. Soc. Am. **81**, 1307–1322 (1987).
[3] E. G. Williams and H. D. Dardy, ''Generalized nearfield acoustical holography for cylindrical geometry: Theory and experiment,'' J. Acoust. Soc. Am. **81**, 389–407 (1987).
[4] B. K. Gardner and R. J. Bernhard, ''A noise source identification technique using an inverse Helmholtz integral equation method,'' J. Vib. Acoust. Stress Reliab. Design **110**, 84–90 (1988).
[5] W. A. Veronesi and J. D. Maynard, ''Digital holographic reconstruction of sources with arbitrarily shaped surfaces,'' J. Acoust. Soc. Am. **85**, 588–598 (1989).
[6] M. R. Bai, ''Application of BEM (boundary element method)-based acoustic holography to radiation analysis of sound sources with arbitrarily shaped geometries,'' J. Acoust. Soc. Am. **92**, 533–549 (1992).
[7] B. K. Kim and J. G. Ih, ''On the reconstruction of the vibro-acoustic field over the surface enclosing an interior space using the boundary element method,'' J. Acoust. Soc. Am. **100**, 3003–3015 (1996).
[8] J. G. Ih and B. K. Kim, ''On the use of the BEM-based NAH for the vibro-acoustic source imaging on the nonregular exterior surfaces,'' Proceedings of Noise-Con 98, Ypsilanti, Michigan, pp. 665–770.
[9] S. F. Wu and J. Yu, ''Reconstructing interior acoustic pressure field via Helmholtz equation least-squares method,'' J. Acoust. Soc. Am. **104**, 2054–2060 (1998).
[10] S. F. Wu and Y. Wu, ''Reconstruction of radiated acoustic pressure fields from a complex vibrating structure,'' Proceedings of the ASME Noise Control and Acoustics Division, ASME, 1998, Vol. 25, pp. 339–345.
[11] D. C. Kammer, ''Sensor placement for on-orbit model identification and correlation of large space structures,'' J. Guid. Control Dyn. **14**, 251–259 (1991).
[12] D. C. Kammer, ''Effect of model error on sensor placement for on-orbit modal identification of large space structures,'' J. Guid. Control Dyn. **15**, 334–341 (1992).
[13] W. H. Press, S. A. Teukolsky, W. T. Vetterling, and B. P. Flannery, *Numerical Recipes in FORTRAN—The Art of Scientific Computing*, 2nd ed. (Cambridge University Press, Cambridge, 1987).
[14] N. Vlahopoulos and S. T. Raveerdra, ''Formulation, implementation, and validation of multiple connection and free edge constraints in an indirect boundary element formulation,'' J. Sound Vib. **210**, No. 1, 137–152 (1998).
[15] J. P. Coyette and K. R. Fyfe, ''Solution of elasto-acoustic problems using a variational finite element/boundary element technique,'' Numerical Techniques in Acoustic Radiation, Proceedings of Winter Annual Meeting of the ASME, San Francisco, Dec. 1989, pp. 15–25.
[16] S. T. Raveendra, N. Vlahopoulos, and A. Glaves, ''An indirect boundary element formulation for multi-valued impedance simulation in structural acoustics,'' Appl. Math. Model. **22**, 379–393 (1998).
[17] S. G. Mikhlin, *Variational Methods in Mathematical Physics* (MacMillan, New York, 1964).
[18] G. Strang, *Linear Algebra and its Applications*, 2nd ed. (Academic, New York, 1980).